expected because larger wire diameter facilitates the formation of multidomains, hence degrading the coercivity. For wire diameters less than 50 nm, the coercivity in some cases becomes smaller. This decrease may be due to the imperfections in the nanostructure. These results also suggest that coercivity can be further enhanced by improving the process for fabricating wires with diameter less than 50 nm.

Perpendicular magnetic recording has been a field under intense exploration. By having their preferred magnetization perpendicular to the film plane, magnetic media with perpendicular anisotropy can allow a smaller bit size to be used and thus increase the recording density (*15*). For a magnetic medium, it is desirable that it be resistant to magnetization reversal, that is, the coercivity should be moderately large. It is also desirable that the remnant magnetization (the magnetization that persists even when the field is absent) be large. As shown in Fig. 4, the magnetic nanowire arrays studied in this work exhibit high perpendicular anisotropy because of their artificial structure. In Fig. 5, we plot the wire diameter dependence of the squareness, which is the ratio of the remanence to saturation magnetization. As expected, the perpendicular squareness is much larger than the parallel squareness. In the case of both Co and Ni nanowires, the perpendicular squareness increases as the wire diameter decreases. The 30-nm Ni nanowire array retains as much as 90% of the magnetization at zero field. The high remanence, together with large coercivities, may make these materials useful for high-density perpendicular recording.

The significance of artificially created one-dimensional structures is much more far reaching than the novel magnetism of the magnetic nanowires studied in this work. One-dimensional structures composed of other suitable materials can also be anticipated to exhibit characteristics of both fundamental (*7*) and practical (*16*) interest.

REFERENCES AND NOTES

1. See, for example, P. Dhez and C. Weisbuch, Eds., *Physics, Fabrication, and Applications of Multilayer Structures* (Springer, Berlin, 1990).
2. M. N. Baibich *et al.*, *Phys. Rev. Lett.* **61**, 2472 (1988).
3. S. S. P. Parkin, N. More, K. P. Roche, *ibid.* **64**, 2304 (1990).
4. B. Abeles, in *Applied Solid State Science: Advances in Materials and Device Research*, R. Wolfe, Ed. (Academic Press, New York, 1976), pp. 1–117, and references therein.
5. C. L. Chien, *J. Appl. Phys.* **69**, 5267 (1991), and references cited therein.
6. G. E. Possin, *Rev. Sci. Instrum.* **41**, 772 (1970).
7. W. D. Williams and N. Giordano, *Phys. Rev. B* **33**, 8146 (1986).
8. B. E. Fischer and D. Spohr, *Rev. Mod. Phys.* **55**, 907 (1983); R. L. Fleischer, P. B. Price, R. M. Walker, *Nuclear Tracks in Solids Principles and Applications* (Univ. of California Press, Berkeley, 1975).
9. P. B. Price and R. M. Walker, *J. Appl. Phys.* **33**, 3407 (1962).
10. T. M. Whitney, thesis, Johns Hopkins University (1992).
11. The nickel was electrodeposited from the following solution: 20 g/liter $NiCl_2 \cdot 6H_2O$, 515 g/liter $Ni(H_2NSO_3)_2 \cdot 4H_2O$, and 20 g/liter H_3BO_3; pH 3.4.
12. The cobalt was electrodeposited from 252 g/liter $CoSO_4 \cdot 7H_2O$, 7 g/liter NaCl, and 50 g/liter H_3BO_3; pH 3.6.
13. See, for example, A. H. Morrish, *The Physical Principles of Magnetism* (Wiley, New York, 1965).
14. For a recent review, see U. Gradmann, *J. Magn. Magn. Mater.* **54–57**, 733 (1986).
15. S. Iwasaki and K. Ouchi, *IEEE Trans. Magn.* **MAG-13**, 1272 (1977).
16. M. Shiraki, Y. Wakui, T. Tokushima, N. Tsuya, *ibid.* **MAG-21**, 1465 (1985); N. Tsuya *et al.*, *ibid.* **MAG-22**, 1140 (1986); K. I. Arai, Y. Wakui, K. Ohmori, T. Tokoshima, *ibid.* **MAG-23**, 2245 (1987).

17. We gratefully acknowledge the assistance of J. M. Macaulay in providing the SEM images. This work was supported by the National Science Foundation under grant ECS 92-02222.

14 April 1993; accepted 12 July 1993

DNA Conformation–Induced Activation of an Enediyne for Site-Specific Cleavage

Lizzy S. Kappen and Irving H. Goldberg*

Neocarzinostatin chromophore (NCS chrom) was found to induce site-specific cleavage at the 3′ side of a bulge in single-stranded DNA in the absence of thiol. This reaction involved the oxidative formation of a DNA fragment with a nucleoside 5′-aldehyde at its 5′ terminus and generated an ultraviolet light–absorbing and fluorescent species of post-activated drug containing tritium abstracted from the carbon at the 5′ position of the target nucleotide. The DNAs containing point mutations that disrupt the bulge were not cleavage substrates and did not generate this drug product. Thus, DNA is an active participant in its own destruction, and NCS chrom may be useful as a probe for bulged structures in nucleic acids.

Neocarzinostatin chromophore (NCS-chrom) (*1*), like the other enediyne anticancer antibiotics calicheamicin (*2*), esperamicin (*3*), and kedarcidin (*4*), is activated for the cleavage of duplex DNA by reaction with thiol. Nucleophilic addition of thiol at C-12 of NCS-chrom (Fig. 1A) results in cycloaromatization of the drug through a Bergman-type reaction to generate the diradical species (*5*). Sequence-specific hydrogen atom abstraction by the diradical from the C-5′, C-1′, or C-4′ positions of deoxyribose in the minor groove of double-stranded (ds) DNA ultimately leads to strand cleavage (*1*). This cleavage is at least 1000 times greater in the presence of thiol than in its absence. Single-stranded (ss) DNA is not a substrate for thiol-activated enediynes except, as shown for NCS-chrom, where regions of ds structure can be generated intramolecularly (*6*, *7*). Here, we report that a ssDNA that contains a bulge is cleaved efficiently and in a site-specific manner by NCS-chrom in the absence of activating thiol; a new drug product results from this reaction.

We found that treatment of ssDNA that corresponded to the 3′ terminus of yeast transfer RNA ($tRNA^{Phe}$) (31-I; Fig. 1B) with NCS-chrom in the absence of thiol (*8*) resulted in cleavage at a single site, T22 (Fig. 2A). This observation suggested that the radical form of NCS-chrom acts monofunctionally in cleaving the DNA. By contrast, dsDNA was not cleaved under these conditions. In the presence of thiol, NCS-chrom induced breaks in both ds- and ssDNAs, predominantly at T and A residues. The mobility of the T22 band in relation to chemical markers and its reduced mobility after exposure to the 3′-phosphatase activity of polynucleotide kinase suggested that the DNA fragment contained a 3′ terminal phosphate. Cleavage was not enhanced by piperidine treatment. Thiol-independent cleavage at T22 in the ss 31-I DNA was dependent on O_2; in its absence, a product (presumably a DNA-drug adduct) that migrated slower than the starting material was formed in an amount comparable to the amount of cleavage product formed in the presence of O_2 (*9*). Thus, drug activation takes place anaerobically, but cleavage of the DNA is an oxidative reaction.

The chemistry of damage at the 5′ end of the break at T22 in the thiol-independent reaction was revealed in experiments with 3′ ^{32}P-labeled ss 31-I (Fig. 2B). Treatment with NCS-chrom produced a band with electrophoretic mobility characteristics consistent with those of a DNA fragment that contained a nucleoside 5′-aldehyde at its 5′ end. Thus, the predominant band (a) moved 3.5 nucleotides more slowly than the

Department of Biological Chemistry and Molecular Pharmacology, Harvard Medical School, Boston, MA 02115.

*To whom correspondence should be addressed.

marker band at T22, was converted by piperidine treatment to a fragment with a 5′-phosphate (b), moved slightly faster after conversion to the alcohol (thymidine) by $NaBH_4$ treatment (c), was protected from piperidine-induced cleavage by prior $NaBH_4$ treatment, and was oxidized to the faster migrating nucleoside 5′-carboxylic acid by sodium hypoiodite treatment (d) (*10*). These results suggest that, in the absence of thiol, NCS-chrom–induced cleavage occurs exclusively by oxidation at the C-5′ of deoxyribose at T22. The high specificity of cleavage exceeds that described earlier for thiol-dependent, double-stranded lesions generated by NCS-chrom at (AGC)·(GCT) and (AGT)·(ACT) sequences (*1*), as well as that observed with other enediynes (*2–4*). Even at high concentrations (50 μM), calicheamicin γ_1^I or esperamicin A_1 did not cleave 31-I in the absence of thiol.

To determine the minimal structural requirements of the DNA substrate for the thiol-independent reaction, we tested a series of 31-I–based DNA substrates containing various nucleotide deletions, insertions, and single and double point mutations. These experiments (*9*) showed that a 16-mer encompassing nucleotides 10 to 25 of 31-I satisfied the basic substrate structural requirements. This oligomer can be folded into a hairpin structure with an apical loop and a 2–base pair stem hinged to a longer base-paired region by a bulge containing T22 on the 3′ side (Fig. 1B). The DNA is presumably bent at the region of the bulge (*11–13*). The substrate requirement is also satisfied in a duplex DNA that consists of an 8-mer strand and a 6-mer strand and that contains the same two-base bulged structure as in 31-I (*9*).

We tested the effect of a single base change in two competent substrates (Fig. 3). A 22-mer that contained a T23C mutation, which destabilizes the bulged structure, was not cleaved by the drug. By contrast, a 16-mer that contained a T22C mutation (a site within the bulge) was cleaved 60% as efficiently as the parent 16-mer; the site of cleavage remained the same.

To determine whether the DNA substrate directly participates in the activation of NCS-chrom in the absence of thiol, we analyzed reaction mixtures that contained the competent 22-mer substrate and the incompetent 22-mer by high-performance liquid chromatography (HPLC) (*14*). The competent substrate produced a major fluorescent and ultraviolet light–absorbing derivative of the drug that eluted with 46% methanol (Fig. 4A). With the incompetent substrate (Fig. 4B) or with no DNA at all (Fig. 4D), this peak represented <5% of

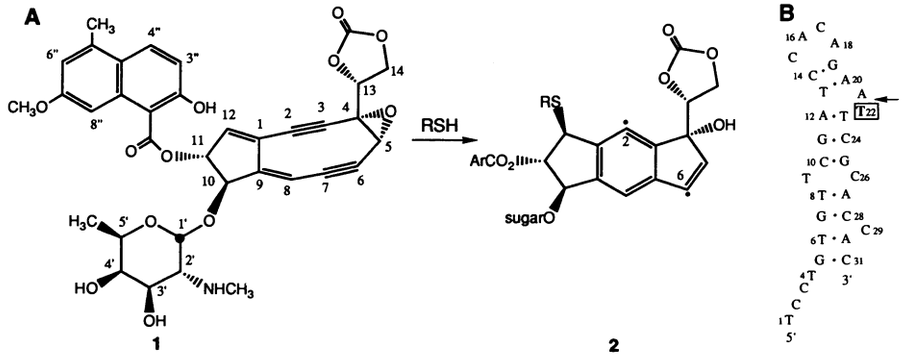

Fig. 1. Drug and DNA structures. (**A**) Thiol activation of NCS-chrom (**1**) to the diradical species (**2**). (**B**) Sequence and proposed conformation of 31-I DNA. Nucleotides correspond to positions 47 to 76 in yeast $tRNA^{Phe}$, which includes the T stem loop. The arrow indicates the side of cleavage at T22. Ar, naphthoate; RSH, any thiol.

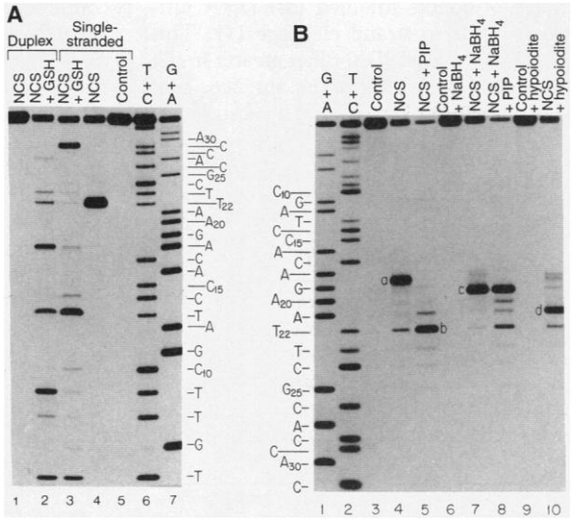

Fig. 2. NCS-chrom–induced cleavage of 31-I DNA. (**A**) Strand cleavage of 5′ ^{32}P-labeled 31-I DNA in the absence or presence of 3 mM glutathione (GSH). Reactions (*8*) contained dsDNA without and with GSH (lanes 1 and 2); ssDNA with GSH, without GSH, and without drug or GSH (lanes 3 to 5); and T + C and G + A sequence markers (lanes 6 and 7). (**B**) Strand cleavage of 3′ ^{32}P-labeled 31-I DNA in the absence of thiol (*8*). Cleaved DNA products (lane 4: nucleoside aldehyde terminus, band a) were subjected to piperidine (PIP) treatment (lane 5: phosphate terminus, band b); reduction with $NaBH_4$ (lane 7: hydroxyl terminus, band c); reduction with $NaBH_4$ followed by PIP treatment (lane 8); or oxidation with hypoiodite (lane 10: carboxylic acid terminus, band d) (*10*). The sequence of 31-I is shown at the side.

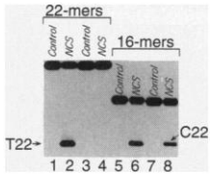

Fig. 3. Effect of a single base change in a competent substrate on NCS-chrom–induced cleavage. Standard reactions were performed in the absence of thiol, with the following 5′ ^{32}P-labeled ssDNA substrates: lanes 1 and 2, 22-mer [C_{10}GATCCACAGAAT$_{22}$TCGCACCAC$_{31}$ (630 μM phosphate)]; lanes 3 and 4, 22-mer with T23C mutation; lanes 5 and 6, 16-mer [C_{10}GATCCACAGAAT$_{22}$TCG (450 μM phosphate)]; and lanes 7 and 8, 16-mer with T22C mutation.

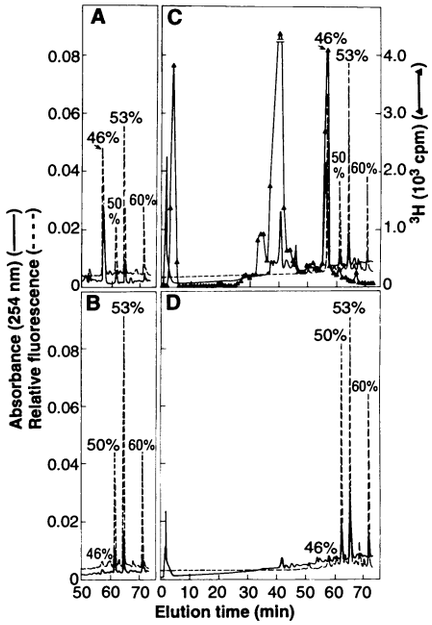

Fig. 4. Detection by HPLC of a post-activated form of NCS-chrom that contained ^3H abstracted from C-5′ of the target nucleotide. (**A**) Competent 22-mer (1.9 mM phosphate). (**B**) Incompetent 22-mer. (**C**) Competent 16-mer (1.35 mM phosphate) that contained a ^3H label at C22 and C24 (49.5 Ci per millimole of ^3H with 42% of the label at the C-5 position and 58% at the C-5′ position). (**D**) NCS-chrom with no DNA. Numbers above the peaks indicate the percentage of methanol in the eluate, and arrows in (A) and (C) indicate the product of DNA-mediated drug activation eluting with 46% methanol.

that produced by the competent substrate. The peaks eluting with 50, 53, and 60% methanol, which represented NCS-chrom spontaneous degradation products, were diminished with the competent substrate. That the new material is the post-activated form of NCS-chrom that is involved in hydrogen atom abstraction from DNA was shown by its incorporation of ^3H when the substrate was a 16-mer DNA with a ^3H label at the C-5′ of C22 (Fig. 4C). These results show that the conversion of NCS-chrom into a hydrogen-abstracting (presumably radical) species requires the participation of a particular DNA structure and confirm the involvement of C-5′ chemistry in the cleavage reaction. Our finding of a new post-activated form of the drug in the presence of bulged DNA contrasts with the thiol-promoted reaction in which the final drug product is the same, whether duplex DNA is present or not (*15*). Radioactive peaks eluting at 4 min and 30 to 45 min represent cytosine (from the partial spontaneous breakdown of nucleoside 5′-aldehyde) and smaller oligonucleotides, respectively, generated in the DNA damage reaction (Fig. 4C). Quantitation of the three radioactive peaks showed that the amount of ^3H abstracted by the drug from C-5′ is sufficient to account for the DNA products.

DNA cleavage involves general base catalysis and is optimal at pH ~9.0. This observation suggests that drug activation requires ionization of the phenolic hydroxyl group of the NCS-chrom naphthoate moiety, which has an equilibrium constant (pK_a) of ~8.5 (*16*). One possibility is that the bent DNA substrate induces a conformational change in NCS-chrom so as to bring the hydroxy naphthoate and the bicyclic enediyne within proximity of the reaction. This change may enhance the ability of a nucleophile, either the phenolate anion or a tautomeric species associated with the naphthoate moiety, to attack C-12 of NCS-chrom and initiate the cycloaromatization reaction to form the radical species (*17*). It is also possible that this reaction is a spontaneous one (*18*) and that a subsequent step is modified by the DNA to generate another intermediate form of the drug.

Our study suggests the potential use of NCS-chrom as a general probe for bulged structures in nucleic acids. The resemblance of the structure studied here and that of the trans-activation response sequence in human immunodeficiency–type 1 viral RNA warrants study of the latter as a target for both natural and synthetic enediynes.

REFERENCES AND NOTES

1. I. H. Goldberg, *Acc. Chem. Res.* **24**, 191 (1991), and references therein.
2. M. D. Lee, G. A. Ellestad, D. B. Borders, *ibid.*, p. 235.
3. Y. Sugiura *et al.*, *Proc. Natl. Acad. Sci. U.S.A.* **86**, 7672 (1989).
4. N. Zein *et al.*, *ibid.* **90**, 2822 (1993).
5. A. G. Myers, *Tetrahedron Lett.* **28**, 4493 (1987).
6. T. Hatayama, I. H. Goldberg, M. Takeshita, A. P. Grollman, *Proc. Natl. Acad. Sci. U.S.A.* **75**, 3603 (1978).
7. L. S. Kappen, C.-q. Chen, I. H. Goldberg, *Biochemistry* **27**, 4331 (1988).
8. A standard reaction (in the dark for 1 hour on ice) contained 50 mM tris-HCl (pH 8.5), 1 mM EDTA, 31-I DNA that was either 5′ ^{32}P-labeled with [γ-^{32}P]adenosine triphosphate and polynucleotide kinase (225 μM phosphate) or 3′ ^{32}P-labeled with [α-^{32}P]cordycepin triphosphate and terminal deoxynucleotidyl transferase (450 μM phosphate), and NCS-chrom (48 μM). NCS-chrom in methanol was added last (final methanol concentration was ≤10%). When dsDNA was the substrate, we annealed the ^{32}P-labeled strand with a 2.5-fold excess of its complementary strand in ×2 reaction buffer by heating the mixture at 90°C for 2 min and cooling it slowly. The dried sample was dissolved in 80% formamide for analysis on a 15% sequencing gel. Gel bands were quantitated with a phosphorimager (Molecular Dynamics, Inc., Sunnyvale, CA). About 73% of the starting material was cleaved at T22.
9. L. S. Kappen and I. H. Goldberg, unpublished data.
10. ———, *Biochemistry* **22**, 4872 (1983).
11. J. A. Rice and D. M. Crothers, *ibid.* **28**, 4512 (1989).
12. A. Bhattacharyya and D. M. Lilley, *Nucleic Acids Res.* **17**, 6821 (1989).
13. C.-H. Hsieh and J. D. Griffith, *Proc. Natl. Acad. Sci. U.S.A.* **86**, 4833 (1989).
14. DNA was first removed from the reaction mixture (200 μl) by ethanol precipitation. The supernatant was lyophilized, and the pellet was redissolved in 10% aqueous methanol for analysis by HPLC with a reversed-phase Beckman Ultrasphere octadecylsilane column (5 μm, 4.6 mm by 25 cm). The column was initially eluted for 10 min (1 ml/min) with 10 mM ammonium acetate (pH 5.0), followed by a 60-min linear gradient of 0 to 60% methanol that contained 10 mM ammonium acetate (pH 5.0). Radioactivity in the fractions was quantitated by liquid scintillation counting.
15. D.-H. Chin, C.-h. Zeng, C. E. Costello, I. H. Goldberg, *Biochemistry* **27**, 8106 (1988).
16. M. A. Napier and I. H. Goldberg, *Mol. Pharmacol.* **23**, 500 (1983).
17. Recent ^1H nuclear magnetic resonance and mass spectroscopic studies of the post-activated drug (O. D. Hensens, D. L. Zink, D.-H. Chin, L. S. Kappen, I. H. Goldberg, unpublished data) indicate that a covalent bond is formed between C-1″ and C-12 as a result of the tautomeric generation of an attacking nucleophile at C-1″.
18. After submission of this paper, M. Lamothe and P. L. Fuchs [*J. Am. Chem. Soc.* **115**, 4483 (1993)] reported on model studies that show that α-hydroxy naphthoate esters can undergo intramolecular alkylation at carbon and both oxygen centers.

19. Supported by U.S. Public Health Service grant CA 44257 from NIH. We thank G. A. Ellestad for calicheamicin γ_1^I and T. W. Doyle and J. Golik for esperamicin A_1.

9 June 1993; accepted 28 July 1993

Rat Annexin V Crystal Structure: Ca^{2+}-Induced Conformational Changes

N. O. Concha,* J. F. Head, M. A. Kaetzel, J. R. Dedman, B. A. Seaton†

Annexins are a family of calcium- and phospholipid-binding proteins implicated in mediating membrane-related processes such as secretion, signal transduction, and ion channel activity. The crystal structure of rat annexin V was solved to 1.9 angstrom resolution by multiple isomorphous replacement. Unlike previously solved annexin V structures, all four domains bound calcium in this structure. Calcium binding in the third domain induced a large relocation of the calcium-binding loop regions, exposing the single tryptophan residue to the solvent. These alterations in annexin V suggest a role for domain 3 in calcium-triggered interaction with phospholipid membranes.

The annexin family of proteins (*1*) is identified by a characteristic amino acid sequence that contains a highly conserved core region, consisting of four or eight repeats of approximately 70 residues, and a highly variable NH_2-terminal region (*2*). The conserved core region gives rise to the Ca^{2+}-dependent binding to phospholipid membranes that is shared by all annexins. The sequence differences found in the NH_2-terminal regions of the molecules may contribute to the specific cellular function of each annexin.

Amino acid sequence data (*3*) indicate that annexins do not have the "E-F hand" Ca^{2+} coordinating sites found in calmodulin and its homologs. Several studies suggest that annexins in the absence of membranes have a much lower (millimolar as compared to micromolar dissociation constants) affinity for Ca^{2+} than the E-F hand family; however, when annexins are bound to the phospholipid bilayer, their apparent Ca^{2+}-binding affinity is greatly enhanced (to micromolar levels) (*4*, *5*). The binding of annexins to phospholipids appears to require a membrane or micelle structure,

N. O. Concha, J. F. Head, B. A. Seaton, Department of Physiology, Boston University School of Medicine, Boston, MA 02118.
M. A. Kaetzel and J. R. Dedman, Department of Physiology and Biophysics, University of Cincinnati College of Medicine, Cincinnati, OH 45267.
*Present address: Center for Advanced Research in Biotechnology, University of Maryland, Rockville, MD 20850.
†To whom correspondence should be addressed.